Biomaterials 33 (2012) 2754–2761

Contents lists available at SciVerse ScienceDirect

Biomaterials

journal homepage: www.elsevier.com/locate/biomaterials

Functional delivery of DNAzyme with iron oxide nanoparticles for hepatitis C virus gene knockdown

Soo-Ryoon Ryoo [d], Hongje Jang [d], Ki-Sun Kim [b], Bokhui Lee [b], Kyung Bo Kim [b], Young-Kwan Kim [d], Woon-Seok Yeo [c], Younghoon Lee [d,***], Dong-Eun Kim [b,**], Dal-Hee Min [a,*]

[a] Department of Chemistry, Seoul National University, Seoul 151-747, Republic of Korea
[b] Department of Bioscience and Biotechnology, WCU and BRL Program, Konkuk University, Seoul 143-701, Republic of Korea
[c] Department of Bioscience and Biotechnology, WCU Program, Konkuk University, Seoul 143-701, Republic of Korea
[d] Department of Chemistry, Korea Advanced Institute of Science and Technology (KAIST), Daejeon 305-701, Republic of Korea

ARTICLE INFO

Article history:
Received 29 November 2011
Accepted 6 December 2011
Available online 27 December 2011

Keywords:
DNAzyme
Drug delivery
Magnetic nanoparticle
Virus

ABSTRACT

DNAzyme is an attractive therapeutic oligonucleotide which enables cleavage of mRNA in a sequence-specific manner and thus, silencing target gene. A particularly important challenge in achieving the successful down-regulation of gene expression is to efficiently deliver DNAzymes to disease sites and cells. Here, we report the nanoparticle-assisted functional delivery of therapeutic DNAzyme for the treatment of hepatitis C by inducing knockdown of hepatitis C virus (HCV) gene, NS3. HCV NS3 gene encodes helicase and protease which are essential for the virus replication. The nanocomplex showed efficient NS3 knockdown while not evoking undesired immune responses or notable cytotoxicity. We also demonstrated the DNAzyme conjugated nanoparticle system could be applicable *in vivo* by showing the accumulation of the nanoparticles in liver, and more specifically, in hepatocytes. We believe that the present work is a successful demonstration of effective, functional, non-immunostimulatory DNAzyme delivery system based on inorganic nanoparticles with high potential for further therapeutic application of DNAzyme in the treatment of hepatitis C.

© 2011 Elsevier Ltd. All rights reserved.

1. Introduction

Down-regulation of mutant genes via gene therapy is a potential strategy for the treatment of many diseases, including genetic disorders, cancers, and virus infections [1–4]. Candidate drugs for gene therapy include various kinds of oligonucleotides, such as short interfering RNA (siRNA) [5], antisense oligonucleotides [6,7], ribozymes [8,9], and deoxyribozymes (DNAzymes) [10,11]. DNAzymes are particularly attractive as gene-silencing agents. They offer several advantages, including cost-effectiveness, straightforward chemical modification, and relatively high stability in serum compared to RNA [11]. The potential utility of DNAzymes as effective gene therapy agents has been demonstrated by experiments in which DNAzymes acting as sequence-specific "molecular scissors" have been able to modulate gene expression at the post-transcriptional level in various clinically relevant model systems *in vitro* and *in vivo* [10,12,13]. The most well-characterized DNAzyme is the 10–23 DNAzyme (Fig. 1A) [14,15]. The DNAzyme has a catalytic core of a 15 base segment that catalyzes RNA cleavage; its sequence-specificity for the target mRNA is provided by flanking sequences of 6–12 bases that are complementary to the target sequence. In spite of their high potential, the lack of a safe, efficient system for the delivery of DNAzymes to target disease sites and tissues remains a major obstacle to the clinical use of DNAzymes.

Hepatitis C is an infectious liver disease caused by the hepatitis C virus (HCV), a small, enveloped, positive-sense single-stranded RNA virus [16,17]. Current treatment for HCV infection involves combination therapy with interferon-α and ribavirin [18,19], but this treatment is not very effective, is accompanied by serious side effects, including flu-like symptoms, fatigue, depression, and hemolytic anemia, and can cause birth defects [20,21]. Additionally, HCV mutates quickly and exhibits strong drug resistance [22]. Thus, no effective antiviral drug for HCV infection is currently available.

A potential therapeutic strategy for hepatitis C treatment is to use a DNAzyme to cleave the HCV genome, thereby preventing the virus from replicating in its host mammalian cells [23,24]. However, if DNAzymes are to be used as antiviral agents, an efficient and safe system for their delivery must be developed.

* Corresponding author. Fax: +82 2 875 6636.
** Corresponding author. Fax: +82 2 3436 6062.
*** Corresponding author. Fax: +82 42 350 2810.
E-mail addresses: younghoon.lee@kaist.ac.kr (Y. Lee), kimde@konkuk.ac.kr (D.-E. Kim), dalheemin@snu.ac.kr (D.-H. Min).

0142-9612/$ – see front matter © 2011 Elsevier Ltd. All rights reserved.
doi:10.1016/j.biomaterials.2011.12.015

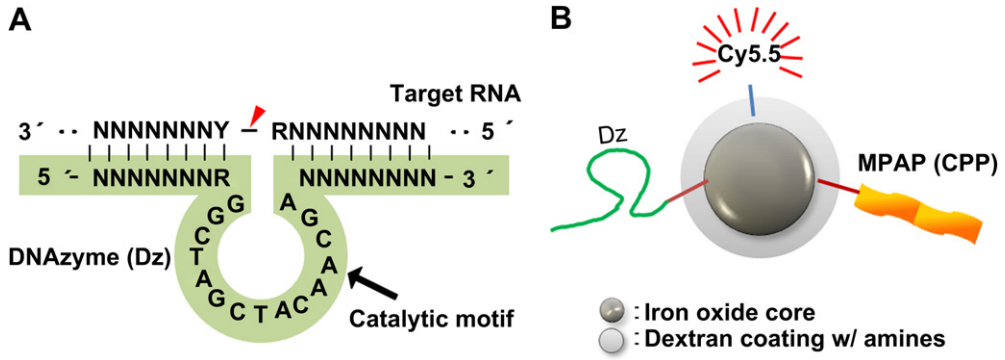

Fig. 1. (A) Structure of the 10–23 synthetic DNAzyme (shaded in green color). A conserved 15 base unpaired motif serves as the catalytic core and is flanked by variable binding domains at its 5′- and 3′-ends. The point of scission within target RNA is indicated by a red color arrow. (B) Multifunctional nanoparticle formulation for DNAzyme delivery. (Dz, DNAzyme; MPAP, myristoylated polyarginine peptide; Cy5.5, fluorescent dye; CPP, cell-penetrating peptide). (For interpretation of the references to colour in this figure legend, the reader is referred to the web version of this article.)

Here, we report an iron oxide nanoparticle-based system for the delivery of DNAzymes to treat hepatitis C. The iron oxide nanoparticles have a magnetic core, coated with dextran, and are conjugated to a synthetic DNAzyme (designated Dz) targeting a gene of interest, a near-infrared fluorescent dye (Cy5.5), and a cell-penetrating peptide (CPP) that aids in membrane translocation (Fig. 1B). We used a previously reported Dz sequence shown to bind to and cleave HCV genomic RNA in the region encoding the non-structural protein 3 (NS3, 70 kDa) [25]. NS3 has long been considered a potential target for anti-HCV therapy because its serine protease and helicase activities are essential for processing of HCV proteins, and it is thus required for HCV replication [26,27]. The conjugated Cy5.5 dye enables tracking of the therapeutic nanoparticle *in vitro* and *in vivo* using fluorescence imaging, and the iron oxide core can be used for tracking via non-invasive magnetic resonance imaging.

2. Methods

2.1. Materials

Dextran (from Leuconostoc ssp., Mr ~ 15 000–25 000) was purchased from Fluka Chemical Corp. (Milwaukee, WI, USA). $FeCl_3 \cdot 6H2O$ and $FeCl_2 \cdot 4H2O$ were purchased Sigma-Aldrich (www.sigma-aldrich.com). DTT (DL-dithiothreitol, 99%) and MTT (3-(4,5-dimethylthiazol-2-yl)-2,5-diphenyl tetrazolium bromide) were purchased from Sigma Chemical Co. (St. Louis, MO, USA). SPDP (N-Succinimidyl-3-(2-Pyridyldithio) Propionate) was purchased from Pierce (Rockford, IL, USA). 10X PBS (Phosphate-Buffered Saline. 10X), DMEM (Dulbecco's Modified Eagle's Medium) and FBS (fetal bovine serum) were purchased from WelGENE Inc. (Seoul, Korea). Amicon Ultra centrifuge filter devices (cutoff: 100 kDa) were purchased from Millipore (Billerica, MA, U.S.A.). Minisart RC 25 syringe filters (0.20 um and 0.45 um pore size) were purchased from Sartorius stedim biotech (Goettingen, Germany). Cy5.5 mono-N-hydroxysuccinamide ester (Cy5.5-NHS) was purchased from GE Healthcare (Piscateway, NJ) and sulfo-LC-SPDP was obtained from Thermo Scientific Pierce Protein Research Products. The MPAP (myristoylated polyarginine peptide) was synthesized by using a standard Fmoc solid phase peptide synthesis protocol. Ethanol was purchased from Merck (Darmstadt, Germany). Phosphate-buffered saline (PBS), Dulbecco's Modified Eagle's Medium (DMEM) and fetal bovine serum (FBS) were purchased from WelGENE Inc. (Seoul, Korea). All chemicals were used as received.

DNAzyme which was designed against HCV NS3 and scrambled-sequence control DNAzyme (scDz) were prepared as follows.

HCV scrambled-sequence DNAzyme (HCV sc Dz, 32mer)
5′- GCA TCA AA**G GCT ATG TAC AAC GA**A TGT GTA GA -3′
HCV Dz #6 (31mer)
5′- AAT GGG GA**G GCT AGC TAC AAC GA**G GCT TTG C -3′

(* underlined letters: catalytic motif of DNAzyme)

2.2. Synthesis of dextran-coated magnetic iron oxide nanoparticle (MN)

To synthesize dextran-coated magnetic iron oxide nanoparticles (MN), 1.5 g of dextran (Mr ~ 15000–25000) and 0.21 g of $FeCl_3$ were dissolved in 7 mL of iced distilled water. A solution of $FeCl_2$ was prepared by dissolving 0.08 g of $FeCl_2$ in 1.7 mL of iced distilled water. A 100 mL round bottomed flask was filled with nitrogen. The prepared Fe^{3+}/dextran and Fe^{2+} solutions were injected to the nitrogen charged round bottomed flask by syringes. 0.33 mL of ammonium hydroxide was added to the flask by dropwise on an ice bath. After the addition of ammonium hydroxide, mixed green colored solution was stirred for 10 min, then ice bath and nitrogen gas were removed. The flask was stirred another 60 min at 80 °C, resulting in color change to dark brown. Excess dextran was removed by filtration using Amicon Ultra 100k centrifuge filter. Filtered nanoparticles were washed 4 times with distilled water. Final dex-MIONs were filtered by 0.45 μm pore sized syringe filter, then filtered again by 0.2 μm pore sized syringe filter.

2.3. Crosslinking of MN

To 2 mL of 30 μM dex-MIONs solution, 3.33 mL of 5 M NaOH and 1.33 mL of epichlorohydrin (99%, Aldrich) were added and vortexed vigorously. The mixed solution was shaked for 24 h at 1200 rpm on a table shaker. After the reaction, crosslinked MN (cl-MN) and remaining materials were injected to dialysis cassette for purification. The reservoirs were immersed into distilled water for dialysis.

2.4. Amination of cl-MN

For amination reaction, cl-MN solution was prepared at 5 mg/mL Fe concentration and 30% (v/v) ammonium hydroxide solution was added to the cl-MN to a final ammonium hydroxide concentration of 10% (v/v). The mixed solution was shaken for 24 h at 600 rpm on a table shaker. After reaction, excess ammonium hydroxide was removed by a size exclusion column filled with Sephadex 25G beads.

2.5. Characterization of MNs (using AFM, DLS, zeta potential, P2T assay)

AFM image was taken with an XE-100 (Park system, Korea) with a backside gold coated silicon probe (M to N, Korea). Particle size distribution was determined by a particle size analyzer Plus90 (Brookhaven). SpectraMax Plus^{384} (Molecular Devices, USA) was used to obtain UV–Vis absorption spectra. Zeta potential measurement was carried out by a zeta sizer Nano ZS90 (Malvern, USA). The number of conjugated DNAzyme was analyzed by gel electrophoresis (15% TBE gel) after DTT (100 mM) treatment.

2.6. Preparation of Cy5.5-conjugated MNs

To conjugate Cy5.5 fluorescence dye to MNs, 300 nmol of Cy5.5 was dissolved in anhydrous DMSO and added to 100 nmol of crosslinked, aminated MNs in PBS on ice bath. Mixed solution was allowed to incubate for 24 h at room temperature with shaking at 600 rpm on a table shaker. The mixture was purified by centrifugation at 4000 rpm by Amicon Ultra centrifuge filter (cutoff: 100 kDa). The product was rinsed 4 times with distilled water, re-dispersed in 1X PBS and stored in dark.

2.7. Conjugation of DNAzyme and CPP to Cy5.5 labeled MNs

To conjugate DNAzyme and CPP, 10 μmol of sulfo-LC-SPDP was dissolved in anhydrous DMSO and added to 100 nmol of Cy5.5-MNs. Mixed solution was incubated for 3 h at room temperature with shaking at 600 rpm on a table shaker. The purification was done by size exclusion column (Sephadex G25) with PBS buffer as a running buffer. Then, 1 eq. of CPP and 2.5 eq. of DNAzyme mixture was added to the sulfo-LC-SPDP linked Cy5.5-MNs. After incubating for 24 h at 600 rpm, the reaction mixture was purified by centrifugation at 3000 rpm with Amicon Ultra centrifuge

filter (cutoff:100 kDa). The final product was rinsed 4 times with PBS and re-dispersed in PBS.

2.8. Cell culture

The human hepatoma cell line Huh-7 was grown in Dulbecco's modified minimal essential medium (DMEM) containing 4.5 g/L D-glucose supplemented with 10% FBS (fetal bovine serum), 100 units/mL penicillin, and 100 mg/mL streptomycin at 37 °C at 5% CO_2. In cell lines carrying HCV replicon RNAs, 500 μg/ml of G418 (A.G. Scientific, Inc. USA) was added to the media.

2.9. Transfection of DNAzyme

For transfection of DNAzyme, Huh-7 cells containing the HCV replicon RNA in G481-containing media were plated in a 6-well plate (3×10^5 cells/well) and were grown for 24 h to reach 70–80% cell confluency. Cells were transfected with DNAzyme or control DNA (scrambled DNAzyme) in serum-free media using Lipofectamine™ 2000 (Invitrogen) according to the manufacturer's protocol. After 4 h of incubation, transfection media was replaced with fresh growth media and incubated for 48 h. For the treatment of Dz-conjugated particles, cells were incubated with the nanoparticles (MN, MPAP-MN, Dz-MN, and Dz-MPAP-MN) for 12 h in serum-free media, followed by further incubation for 36 h with fresh growth media.

2.10. Western blotting and semi-quantitative RT-PCR

Total cell lysates were prepared and separated on SDS-PAGE, and transferred onto Immobilon-P membranes (Millipore). The membranes were blocked with 5% skim milk and probed with primary antibody (anti-HCV NS3 (Virostat, USA), PKR (B-10), p-PKR (Thr 446) and anti-β-actin antibodies (Santa Cruz Biotechnology). The membrane was then incubated with horseradish-peroxidase-conjugated secondary antibody (Sigma) and visualized by enhanced chemiluminescence detection system (Pierce).

Total RNA was extracted by using Trizol reagent (Invitrogen) according to the manufacturer's instruction. Total RNA was quantified and the quality of total RNA was analyzed based on the 28S:18S rRNA ratio by using agarose gel electrophoresis. Total RNA samples (2 mg each) were used for reverse transcription under standard conditions (SuperScript II reverse transcriptase; Invitrogen). The resulting cDNA was used as template in subsequent PCR amplifications. Sequences of interest were amplified by using the following primer pairs: HCV NS3 (5′-AGACCA-CAACGGTTTCCCTCTAGA-3′/5′-CTTAATTAATTAGGCCTCTCGAGC-3′), TLR3 (5′-AGC-CACCTGAAGTTGACTCAGG-3′/5′-CAGTCAAATTCGTGCAGAAGGC-3′), and IFN-β (5′-ACCAACAAGTGTCTCCTCCA-3′/5′-GAGGTAACCTGTAAGTCTGT-3′). GAPDH (5′-TTGTTGCCATCAATGACCCCTTCATTGACC-3′/5′-CTTCCCGTTCTCAGCCTTGACGGTG -3′) was used as endogenous reference housekeeping gene. The PCR reaction for HCV NS3 was performed as follows: (30 s at 95 °C, 30 s at 55 °C, 30 s at 72 °C) × 35 cycles. The PCR reaction for TLR3 was performed as follows: (30 s at 94 °C, 30 s at 57 °C, 40 s at 72 °C) × 32 cycles. The condition of PCR reaction for IFN-β was performed as follows: (1 min at 94 °C, 2 min at 60 °C, 3 min at 72 °C) × 35 cycles. The condition of PCR reaction for GAPDH was as follows: 5 min at 94 °C, (30 s at 94 °C, 30 s at 60 °C, 30 s at 72 °C) × 26 cycles. PCR products were separated on a 1% agarose gel and analyzed using a Gel Doc system (Bio-Rad, Hercules, CA). Relative intensity of each band normalized to GAPDH was quantified using NIH ImageJ software.

2.11. Luciferase assay

Huh-7 Luc-Neo cells were transfected as described above ("*Transfection of DNAzyme*"). The cells were washed with 1X PBS and were then lysed with 100uL of 1X Passive Lysis Buffer (PLB) (Promega Corp.) for 15 min at room temperature. Cell lysate (20 μl per condition) was transferred to a 96-well plate; 100 μL of luciferase assay reagent was added per well, and the relative light units were measured after a 2 s delay by a Lumat LB 9501 luminometer (Berthold, Wilbach, Germany). The total protein content of the different samples was quantified to normalize the luciferase reporter assay data. Experiments were done in duplicate. Values were normalized by the total protein content of each sample. Total protein content of whole-cell extract

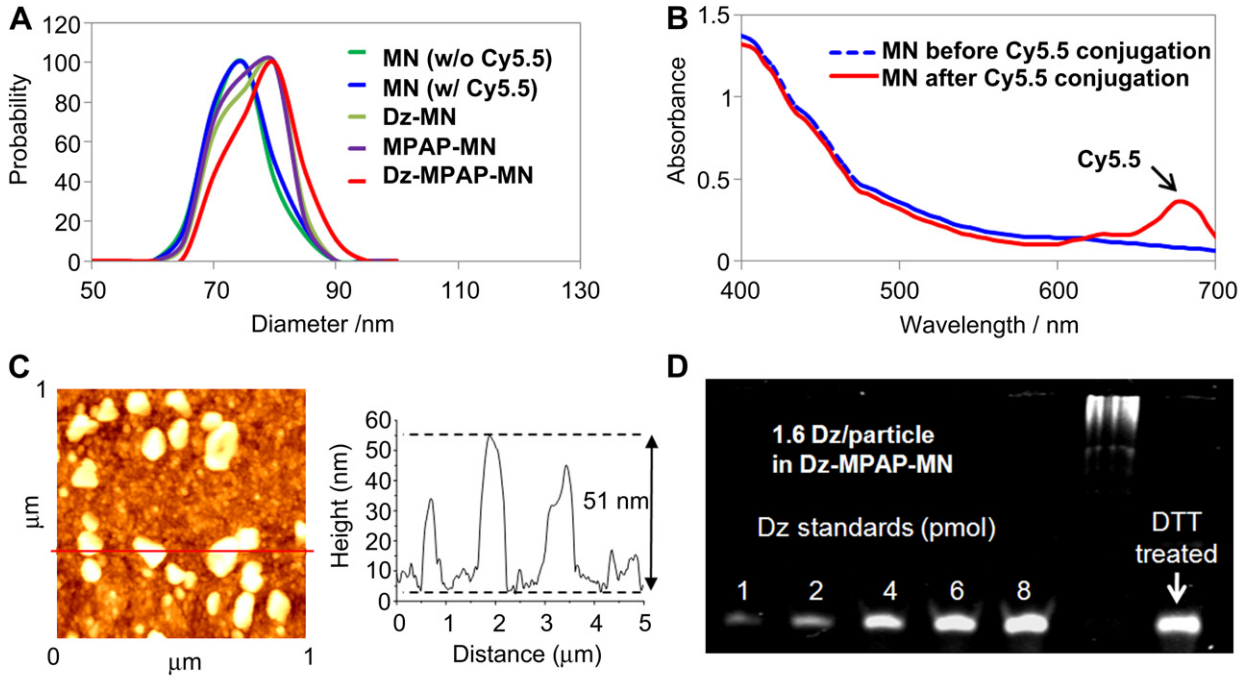

E Zeta potentials (mV)

MN	Cy5.5-MN	Dz-MN	MPAP-MN	Dz-MPAP-MN
(Cross–linked, aminated)	(Cy5.5 conjugated)	(Cy5.5, Dz conjugated)	(Cy5.5, MPAP conjugated)	(Cy5.5, MPAP, Dz conjugated)
7.60	7.48	4.43	10.11	7.25

Fig. 2. Characterization of magnetic iron oxide nanoparticles (MNs). (A) The dynamic light scattering data indicate a mean hydrodynamic diameter of 75–80 nm for the prepared MN species. Colloidal stability was maintained without aggregation even after serial conjugation of Cy5.5, Dz, and MPAP. (B) UV–Vis absorption spectra of the MNs and the Cy5.5-conjugated MNs. (C) Atomic force microscopic analysis showed that the MNs are spherical, with a diameter of ~50 nm. (D) The number of conjugated Dz molecules was analyzed using gel electrophoresis after dithiothreitol (DTT, a reducing agent) treatment. (E) Measured zeta potentials for each nanoparticle species prepared in this study.

lysates was quantified using the Bio-Rad Protein Assay Dye Reagent Concentrate (Bio-Rad Laboratories, Mississauga, Ont.), similar to the well-documented Bradford assay. BSA was used as a protein standard. The absorbance was obtained using a SpectraMax Plus^{384} UV–Vis spectrophotometer (Molecular Devices, USA) at 595 nm after 10 min of incubation at room temperature.

2.12. MTT assay for viability test

Huh-7 cells were seeded at 10,000 cells per well of a 96-well culture plate with 100 mL of growth media (about 50–70% confluency). The MTT (3-(4,5-dimethylthiazol-2-yl)-2,5-diphenyltetrazolium bromide) assay was used to quantify the viability of cells. Cells were incubated with Cy5.5-MNs (at concentrations ranging from 1.45 to 23.2 μM) and incubated for 24 and 48 h at 37 °C. Following Cy5.5-MN treatment, cells were rinsed with 1X PBS and incubated with 20 μl MTT stock solution (5 mg/ml MTT dissolved in 1X PBS) in each well to detect metabolically active cells. The cells were incubated for 2~4 h until the purple color was developed indicating that MTT was to be metabolized. The media were discarded, and 200 μl DMSO was added to each well to make insoluble formazan salt soluble. Then, the optical densities were measured at 560 nm and background absorbance at 670 nm was subtracted.

2.13. In vitro cell internalization

For the observation of internalized MNs, Huh-7 Luc-Neo cells maintained in G481-containing media were plated on the sterile glass inside each well of the 12-well culture plate and grown for 24 h before the nanoparticle treatment ($1\sim2\times10^5$ cells/well). After the nanoparticles (MN, Dz-MN and Dz-MPAP-MN) were treated into the cells for 12 h, the cells were fixed with 4% paraformaldehyde in 1X PBS (pH 7.4) at RT. The fixed cells were washed with 1X PBS and mounted with Vectashield containing DAPI (Vector Labs. USA). The images were observed using a Ti inverted fluorescence microscope.

2.14. Animal experiments for optical imaging analysis

All animal care and experimental procedures were approved by the Animal Care Committees of Korea Advanced Institute of Science and Technology (KAIST). Nude BALB/c mice (4 week old) were obtained from Central Lab Animal Inc. and C57BL/6N mice were obtained from Orient Bio Inc.

3. Results and discussion

We prepared dextran-coated, magnetic iron oxide nanoparticles (MNs), crosslinked the dextran, and aminated the particle surface according to a previously reported method [28,29]. Quantitative measurement of the number of amine groups on the MN surface using a pyridine-2-thione assay [30,31] yielded a value of ~57 amines/particle. The zeta potential of the MNs, which was −5.44 mV before amination, increased to 7.6 mV upon amination. Then, the fluorescent dye Cy5.5 was conjugated to the aminated MNs using Cy5.5 *N*-hydroxylsuccimide ester. As measured by dynamic light scattering, the average hydrodynamic diameter of the Cy5.5-conjugated MNs (Cy5.5–MNs) was 75 nm, similar to that of non-conjugated MNs (Fig. 2A). Successful conjugation of Cy5.5 to the MNs was demonstrated using UV–Visible spectroscopy, which yielded a characteristic Cy5.5 absorption peak at 680 nm for Cy5.5–MN and showed an average of 1.7 Cy5.5 conjugates per MN (Fig. 2B). Analysis by atomic force microscopy showed that the nanoparticles were well-dispersed and spherical, with an overall diameter of about 50 nm (Fig. 2C).

Cy5.5–MNs were conjugated to thiolated Dz and a myristoylated polyarginine peptide (MPAP; myristic acid-ARRRRRRRC), using a cross-linker, sulfosuccinimidyl-6-(3′-(2-pyridyldithio)-propionamido)-hexanoate (sulfo-LC-SPDP). MPAP which acts as a cell-penetrating peptide was used to enhance the efficiency of cellular uptake [32]. In the MN, linked to both Dz and MPAP (DzMPAPMN), Dz and MPAP were attached via a disulfide linkage which can be cleaved in reducing environments, such as that in the cytoplasm [33]. On average, 1.6 Dz molecules were introduced per MN, as determined by electrophoresis of the particles on a 15% Tris-borate-EDTA gel after treatment with a reducing agent (Fig. 2D). The various conjugated MN species had similar average hydrodynamic sizes (75–80 nm) (Fig. 2A). To further characterize these nanoparticles, we measured their zeta potentials; Dz-MPAP-MN and Cy5.5–MN had similar zeta potentials (7.25 and 7.48 mV, respectively), suggesting that the positive and negative charges of the MPAP and Dz moieties were compensated against each other (Fig. 2E).

To demonstrate our strategy for functional DNAzyme delivery, we used Huh-7 Luc-Neo hepatoma cells, which carry a subgenomic HCV replicon (genotype 1b) and a luciferase reporter gene (Huh-7 Luc-Neo cell) [34,35]. To confirm that Dz itself was active in cultured HCV replicon cells, the cells were first transfected with

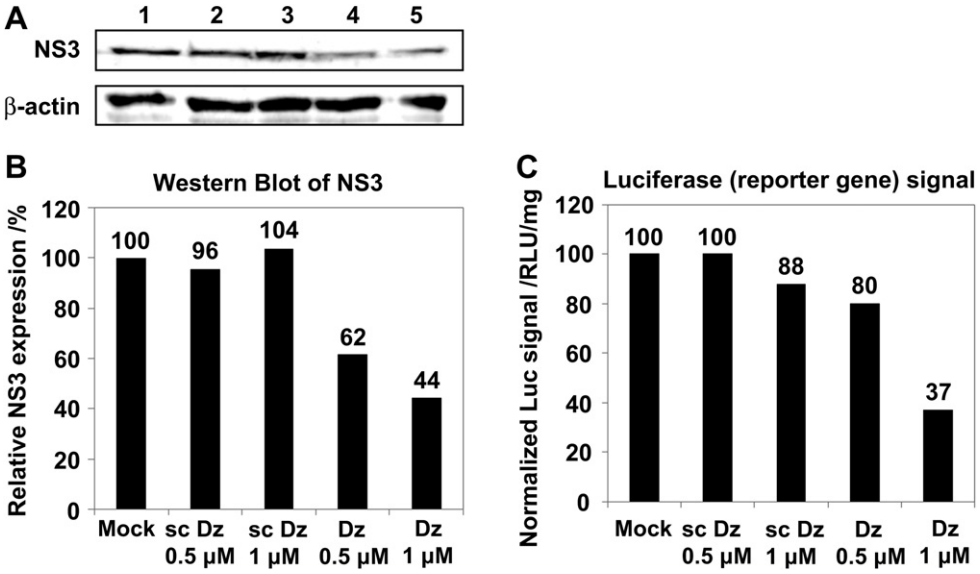

Fig. 3. Analysis of NS3 knockdown efficacy of Dz itself in Huh-7 hepatocytes harboring an HCV replicon (Huh-7 Luc-Neo cells). The cells were transfected with unconjugated Dz using Lipofectamine 2000. Expression of β-actin and HCV NS3 proteins was assessed by (A) Western blotting (1. MOCK; 2. 0.5 μM scrambled Dz (scDz); 3. 1 μM scz; 4. 0.5 μM Dz; 5. 1 μM Dz) and (B) densitometric analysis of the Western blot. Band density values for NS3 were normalized to the β-actin band density. NS3 protein expression was reduced to 44% of that in the mock-treated control when the cells were transfected with 1 μM Dz against NS3. (C) Luciferase (reporter gene) activity in Huh-7 Luc-Neo cells after Dz transfection. Luciferase reporter assay data were normalized to the total protein content of the corresponding samples.

free Dz at various concentrations (0–1 μM) using Lipofectamine 2000. After a 4 h incubation, the medium was replaced with fresh medium. At 48 h post-transfection, NS3 gene-silencing was evaluated using Western blot and luciferase activity analyses. Western blotting confirmed that Dz dose-dependently down-regulated NS3 expression by as much as 56% (Fig. 3A, B). Similarly, the luciferase (reporter) signal for the cells transfected with 1 μM Dz was decreased by 63% (Fig. 3C).

We next evaluated the extent of HCV NS3 gene suppression in HCV replicon cells treated with Dz-conjugated MNs. Cultured Huh-7 Luc-Neo cells were treated with MN, MPAP-MN, Dz-MN, and Dz-MPAP-MN at concentrations up to 1 μM for 12 h. The culture

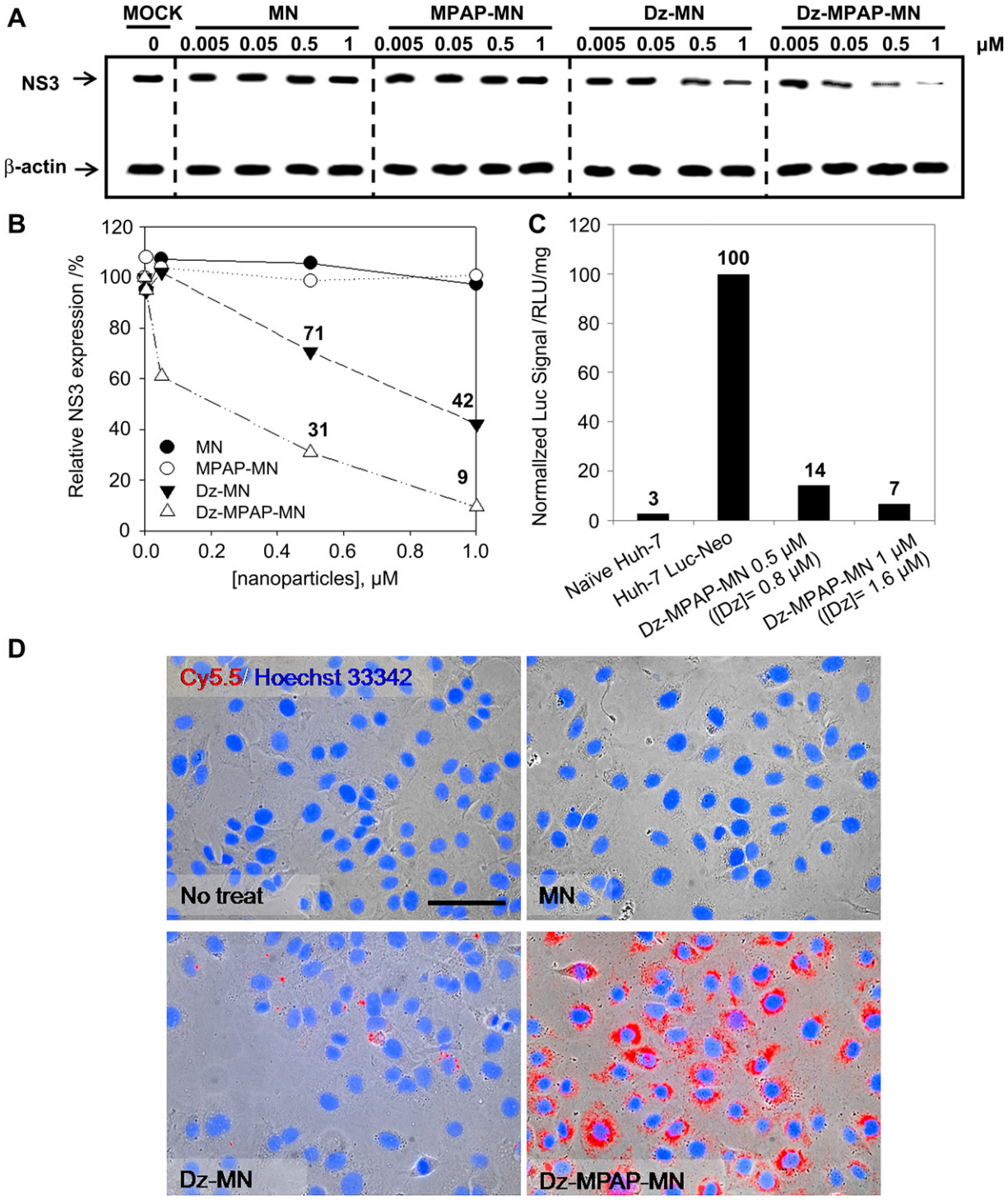

Fig. 4. *In vitro* analysis of NS3-silencing efficiency of Dz-conjugated nanoparticles in Huh-7 Luc-Neo cells. (A) Western blot analysis of HCV NS3 expression in cultured Huh-7 Luc-Neo cells treated with Dz-conjugated multifunctional nanoparticles. (B) Densitometric analysis of the data shown in (a). Density values for NS3 were normalized to the β-actin band density. (C) Luciferase (reporter gene) assays of Huh-7 Luc-Neo cells treated with Dz-MPAP-MN indicate dose-dependent down-regulation of the NS3 target gene. (D) Fluorescence images of Huh-7 Luc-Neo cells taken 12 h after treatment with various MN species (Blue, Hoechst 33342-stained nuclei; red, Cy5.5-conjugated MNs). Cellular uptake efficiency was much higher for the MPAP-conjugated MN than for the MN species lacking MPAP. Nanoparticles inside the cells localized primarily in the perinuclear region. Scale bar is 20 μm. (For interpretation of the references to colour in this figure legend, the reader is referred to the web version of this article.)

medium was then replaced with fresh culture medium, and the cells were incubated for another 36 h. Western blotting showed that both Dz-MN and Dz-MPAP-MN down-regulated NS3 expression dose-dependently (Fig. 4A, B). Quantitative evaluation of the NS3 bands on the Western blot showed that the maximum reduction of NS3 expression (a decrease of 91%) was achieved using 1 μM Dz-MPAP-MN. Cells treated with MN or MPAP-MN showed no appreciable change in NS3 gene expression. In luciferase activity assays of the cells treated with Dz-MPAP-MNs, the amount of luciferase activity followed a downward trend, similar to that observed for NS3 expression by Western blotting, suggesting that the amount of suppression of the luciferase reporter gene is a valid indirect measure of NS3 gene-suppressing activity in this system (Fig. 4C). Uptake of MN, Dz-MN, and Dz-MPAP-MN by the HCV replicon cells was evaluated by Cy5.5 fluorescence microscopy 12 h after MN treatment. As shown in Fig. 4D, Dz-MPAP-MN was most efficiently internalized and accumulated, primarily at the perinuclear region in the Huh-7 cells, whereas MN and Dz-MN were rarely observed inside the cells.

Taken together, these results demonstrate that Dz-conjugated MNs efficiently and dose-dependently suppress the NS3 target gene expression in HCV replicon cells and that the Dz, and not the MPAP or the MN itself, is responsible for this knockdown effect. Also, the addition of the MPAP cell-penetrating peptide to Dz-MN greatly increases the extent of cellular uptake and NS3 knockdown. In fact, Dz-MPAP-MN treatment decreased NS3 expression by an amount even greater than that caused by Lipofectamine 2000-mediated transfection of similar concentrations of Dz. NS3 expression levels decreased to 44% of the control with transfection of 1 μM free Dz and to 31% of the control with internalization of Dz-MPAP-MN at an effective Dz concentration of 0.8 μM (Fig. 3B and Fig. 4B). An even greater difference in NS3 expression was suggested by luciferase reporter assays (37% vs. 14%; Fig. 3C and Fig. 4C), suggesting efficient and functional Dz delivery by the Dz-MPAP-MN formulation.

Cytotoxicity is one consideration in the development of drug delivery systems. Thus, we evaluated Huh-7 cells for cytotoxicity after they were treated with various concentrations of MNs up to

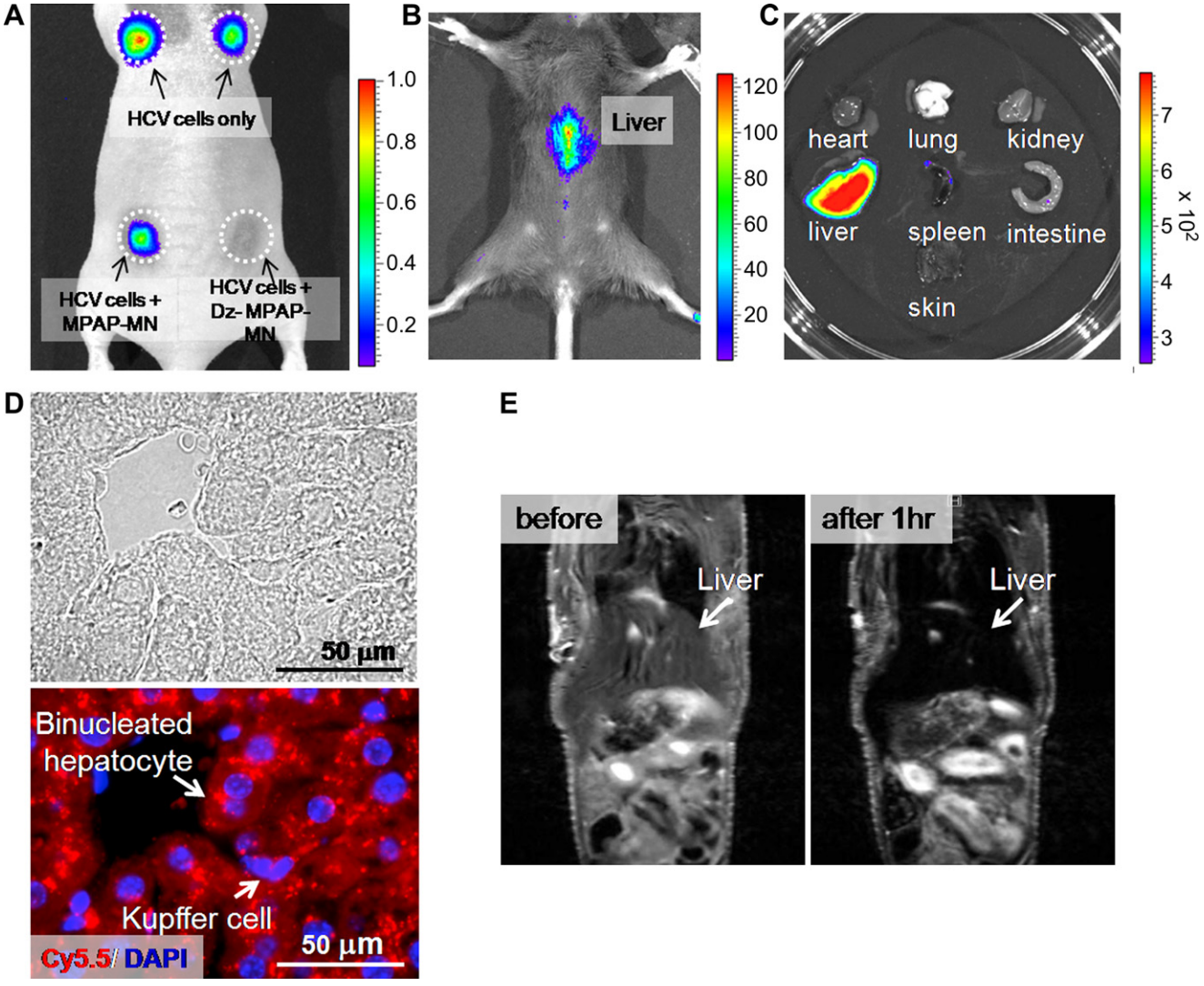

Fig. 5. Analysis of Dz-MPAP-MN efficacy *in vivo* and biodistribution of Dz-MPAP-MN. (A) Dz-MPAP-MN treatment of HCV replicon cells reduced the luciferase signal *in vivo* after subcutaneous injection of the cells into mice. A whole-body luminescence image of a mouse injected with cells treated or not treated with Dz-MPAP-MN shows that the luciferase (reporter) signal is greatly reduced in the treated cells. b–e) Biodistribution of Dz-MPAP-MN after intravenous administration to mice. (B) A whole-body image showing intense Cy5.5 fluorescence in the area of the liver. (C) Fluorescence images of the extracted organs show that the particles accumulate primarily in the liver. Bright field and fluorescence images of the extracted liver tissue slice are shown in (D). Cellular uptake and accumulation of the intravenously injected Dz-MPAP-MNs were observed in both hepatocytes and Kupffer cells. (E) T2-weighted MR images of a mouse before (left) and 1 h after (right) injection of nanoparticles. Accumulation of the nanoparticles in liver is observed.

23 μM (Fig. S1). Using MTT assays, we found little evidence for MN cytotoxicity in the range of effective working concentrations.

We next examined whether our DNAzyme delivery system would elicit an innate immune response *in vitro*. Undesired immune responses are an important consideration in gene therapy and in the development of gene delivery systems because the introduction of exogenous genes can activate the innate immune system of human cells to combat foreign gene or pathogen invasion [36]. For example, siRNA can provoke an immune response via its interactions with Toll-like receptors (TLRs) and trigger an interferon (IFN) response [37,38]. Additionally, systemically introduced lipid nanoparticles have been reported to induce an immune response in mice [39]. Thus, because the potential immunostimulatory properties of a proposed gene delivery system are important, we characterized Huh-7 Luc-Neo cells and naïve Huh-7 cells (lacking the HCV replicon) for their innate immune response to the nanoparticle complexes. We measured the expression of TLR3 and IFN-β using semi-quantitative reverse transcriptase (RT)-PCR and measured the extent of phosphorylation of double-stranded RNA-activated protein kinase R (PKR) [40] using Western blotting. No appreciable signal corresponding to TLR3, IFN-β, or phosphorylated PKR was observed on treatment of naïve Huh-7 cells with MN, MPAP-MN, or Dz-MPAP-MN (Fig. S2A). On the other hand, the HCV replicon-containing cells exhibited some degree of TLR3 and IFN-β expression and PKR phosphorylation even in the absence of treatment, probably because of the foreign replicon in the cells (Fig. S2B). Upon treatment with Dz-conjugated nanoparticles, both the expression of TLR3 and IFN-β and the degree of phosphorylation of PKR decreased as NS3 expression also decreased, suggesting that Dz-MPAP-MN itself does not elicit on Huh-7 cells appreciable innate immune responses *in vitro*.

To examine the efficacy of the Dz-conjugated nanoparticles *in vivo*, we injected mice subcutaneously with Dz-MPAP-MN-treated Huh-7 replicon cells. Although the ideal test for the *in vivo* efficacy of drug-loaded nanoparticles would use a virus-infected animal model, small animals (e.g., mice) are not susceptible to infection by human viruses, such as HIV-1 and HCV. Indeed, HCV infects only humans and chimpanzees [41,42]. In fact, generating xenograft tumors of the HCV replicon Huh-7 cells was not straightforward; the subcutaneously injected cells rapidly lost all of their luciferase activity, within 4 days, because the host rejection process rapidly eliminated the replicon RNA [43]. In our experiments, the luciferase signal from the whole mouse body was measured 24 h after the injection of 4×10^6 HCV replicon cells with or without MPAP-MN (18.09 μM) or Dz-MPAP-MN (15.08 μM). The mice were peritoneally injected with luciferin (1.5 mg/10 g body weight) immediately before imaging. As seen in the whole mouse image in Fig. 5A, the cells co-injected with Dz-MPAP-MN exhibited a lower luciferase signal than the controls, suggesting that Dz-MPAP-MN may effectively down-regulates its target gene *in vivo*.

For practical application of systemically introduced nanoparticles, the particles should accumulate in the liver, the site of Dz function. When mice were injected with Dz-MPAP-MN via their tail veins, the particles were found exclusively in the liver within 30 min after injection, as shown by Cy5.5 fluorescence imaging of the nanoparticles and *ex vivo* imaging after organ extraction (Fig. 5B, C). Examination of liver tissue sections by fluorescence microscopy showed that the injected particles were taken up by both hepatocytes and Kupffer cells (liver macrophages) in the liver. The accumulation of the particles in both types of cells, rather than just in the Kupffer cells, is an encouraging sign for their potential use for hepatitis C treatment (Fig. 5D). In addition, MR images taken before and after nanoparticle injection showed that the nanoparticles were mainly accumulated in the liver as expected, demonstrating that the multifunctional nanoparticles could be used as an effective T2 MRI contrast agent for tracing DNAzyme delivery vehicles *in vivo* (Fig. 5E).

4. Conclusion

We have successfully demonstrated a new functional DNAzyme delivery system that harnesses well-characterized iron oxide nanoparticles to effectively silence expression of the HCV NS3 gene. The nanoparticle complex does not provoke undesired immune responses in Huh-7 cells *in vitro* and has a higher knockdown efficacy than the free DNAzyme transfected with Lipofectamine 2000. DNAzymes are attractive therapeutic candidates because (1) their ability to cleave RNA substrates in a sequence-specific manner can be used to silence target genes, (2) they are much more stable than ribozymes, and (3) they are less expensive than siRNA molecules. The present study is a successful demonstration of an effective, functional DNAzyme delivery system with a high potential for future clinical use in the treatment of hepatitis C. This inorganic nanoparticle-based DNAzyme delivery system may be readily extended to accommodate other hepatitis C drugs, e.g., small-molecule inhibitors of HCV polymerase, NS3 protease, or NS3 helicase activity, in addition to DNAzymes in the future; the loading of multiple entities onto nanoparticles may provide a synergistic therapeutic effect.

Acknowledgments

This work was supported by the National Research Foundation of Korea (NRF), funded by the Korean government (the Ministry of Education, Science and Technology, MEST) (Grant Nos. 313-2008-2-C00538, 2008-0062074, 2011-0020322, 2011-0017356), by the Nano R&D program of NRF funded by MEST (2008-2004457), and by the National Honor Scientist Program of MEST, Korea. We thank Dr. Jee-Hyun Cho for helping in obtaining MRI at the Korea Basic Science Institute in Ochang.

Appendix. Supplementary material

Supplementary data related to this article can be found online at doi:10.1016/j.biomaterials.2011.12.015.

References

[1] Li SD, Huang L. Gene therapy progress and prospects: non-viral gene therapy by systemic delivery. Gene Ther 2006;13:1313–9.
[2] Bunnell BA, Morgan RA. Gene therapy for infectious diseases. Clin Microbiol Rev 1998;11:42–56.
[3] McCormick F. Cancer gene therapy: fringe or cutting edge? Nat Rev Cancer 2001;1:130–41.
[4] Kim DH, Rossi JJ. Strategies for silencing human disease using RNA interference. Nat Rev Genet 2007;8:173–84.
[5] Medarova Z, Pham W, Farrar C, Petkova V, Moore A. In vivo imaging of siRNA delivery and silencing in tumors. Nat Med 2007;13:372–7.
[6] Askari FK, McDonnell WM. Antisense-oligonucleotide therapy. N Engl J Med 1996;334:316–8.
[7] McClorey G, Moulton HM, Iversen PL, Fletcher S, Wilton SD. Antisense oligonucleotide-induced exon skipping restores dystrophin expression in vitro in a canine model of DMD. Gene Ther 2006;13:1373–81.
[8] Bai Y, Gong H, Li H, Vu GP, Lu S, Liu F. Oral delivery of RNase P ribozymes by Salmonella inhibits viral infection in mice. Proc Natl Acad Sci USA 2011;108:3222–7.
[9] Vaish NK, Kore AR, Eckstein F. Recent developments in the hammerhead ribozyme field. Nucleic Acids Res 1998;26:5237–42.
[10] Dass CR, Choong PF, Khachigian LM. DNAzyme technology and cancer therapy: cleave and let die. Mol Cancer Ther 2008;7:243–51.
[11] Appaiahgari MB, Vrati S. DNAzyme-mediated inhibition of Japanese encephalitis virus replication in mouse brain. Mol Ther 2007;15:1593–9.
[12] Achenbach JC, Chiuman W, Cruz RP, Li Y. DNAzymes: from creation in vitro to application in vivo. Curr Pharm Biotechnol 2004;5:321–36.
[13] Dass CR. Deoxyribozymes: cleaving a path to clinical trials. Trends Pharmacol Sci 2004;25:395–7.
[14] Santoro SW, Joyce GF. A general purpose RNA-cleaving DNA enzyme. Proc Natl Acad Sci USA 1997;94:4262–6.

[15] Santoro SW, Joyce GF. Mechanism and utility of an RNA-cleaving DNA enzyme. Biochemistry 1998;37:13330–42.
[16] Choo QL, Kuo G, Weiner AJ, Overby LR, Bradley DW, Houghton M. Isolation of a cDNA clone derived from a blood-borne non-A, non-B viral hepatitis genome. Science 1989;244:359–62.
[17] Lindenbach BD, Rice CM. Unravelling hepatitis C virus replication from genome to function. Nature 2005;436:933–8.
[18] Reichard O, Norkrans G, Fryden A, Braconier JH, Sonnerborg A, Weiland O. Randomised, double-blind, placebo-controlled trial of interferon alpha-2b with and without ribavirin for chronic hepatitis C. The Swedish Study Group. Lancet 1998;351:83–7.
[19] Bizollon T, Palazzo U, Ducerf C, Chevallier M, Elliott M, Baulieux J, et al. Pilot study of the combination of interferon alfa and ribavirin as therapy of recurrent hepatitis C after liver transplantation. Hepatology 1997;26:500–4.
[20] Kowdley KV. Hematologic side effects of interferon and ribavirin therapy. J Clin Gastroenterol 2005;39:S3–8.
[21] Schaefer M, Schmidt F, Folwaczny C, Lorenz R, Martin G, Schindlbeck N, et al. Adherence and mental side effects during hepatitis C treatment with interferon alfa and ribavirin in psychiatric risk groups. Hepatology 2003;37:443–51.
[22] Kuntzen T, Timm J, Berical A, Lennon N, Berlin AM, Young SK, et al. Naturally occurring dominant resistance mutations to hepatitis C virus protease and polymerase inhibitors in treatment-naive patients. Hepatology 2008;48:1769–78.
[23] Roy S, Gupta N, Subramanian N, Mondal T, Banerjea AC, Das S. Sequence-specific cleavage of hepatitis C virus RNA by DNAzymes: inhibition of viral RNA translation and replication. J Gen Virol 2008;89:1579–86.
[24] Kumar D, Chaudhury I, Kar P, Das RH. Site-specific cleavage of HCV genomic RNA and its cloned core and NS5B genes by DNAzyme. J Gastroenterol Hepatol 2009;24:872–8.
[25] Lee B, Kim KB, Oh S, Choi JS, Park JS, Min D-H, et al. Suppression of hepatitis C virus genome replication in cells with RNA-cleaving DNA enzymes and short-hairpin RNA. Oligonucleotides 2010;20:285–96.
[26] Frick DN. The hepatitis C virus NS3 protein: a model RNA helicase and potential drug target. Curr Issues Mol Biol 2007;9:1–20.
[27] Maga G, Gemma S, Fattorusso C, Locatelli GA, Butini S, Persico M, et al. Specific targeting of hepatitis C virus NS3 RNA helicase. discovery of the potent and selective competitive nucleotide-mimicking inhibitor QU663. Biochemistry 2005;44:9637–44.
[28] Molday RS, MacKenzie D. Immunospecific ferromagnetic iron-dextran reagents for the labeling and magnetic separation of cells. J Immunol Methods 1982;52:353–67.
[29] Josephson L, Tung CH, Moore A, Weissleder R. High-efficiency intracellular magnetic labeling with novel superparamagnetic-Tat peptide conjugates. Bioconjug Chem 1999;10:186–91.
[30] Zhao M, Kircher MF, Josephson L, Weissleder R. Differential conjugation of tat peptide to superparamagnetic nanoparticles and its effect on cellular uptake. Bioconjug Chem 2002;13:840–4.
[31] Ngo TT. A simple spectrophotometric determination of solid supported amino groups. J Biochem Biophys Method 1986;12:349–54.
[32] Nelson AR, Borland L, Allbritton NL, Sims CE. Myristoyl-based transport of peptides into living cells. Biochemistry 2007;46:14771–81.
[33] Saito G, Swanson JA, Lee KD. Drug delivery strategy utilizing conjugation via reversible disulfide linkages: role and site of cellular reducing activities. Adv Drug Deliv Rev 2003;55:199–215.
[34] Pietschmann T, Lohmann V, Rutter G, Kurpanek K, Bartenschlager R. Characterization of cell lines carrying self-replicating hepatitis C virus RNAs. J Virol 2001;75:1252–64.
[35] Lohmann V, Hoffmann S, Herian U, Penin F, Bartenschlager R. Viral and cellular determinants of hepatitis C virus RNA replication in cell culture. J Virol 2003;77:3007–19.
[36] Aderem A, Ulevitch RJ. Toll-like receptors in the induction of the innate immune response. Nature 2000;406:782–7.
[37] Kariko K, Bhuyan P, Capodici J, Weissman D. Small interfering RNAs mediate sequence-independent gene suppression and induce immune activation by signaling through toll-like receptor 3. J Immunol 2004;172:6545–9.
[38] Marques JT, Williams BR. Activation of the mammalian immune system by siRNAs. Nat Biotechnol 2005;23:1399–405.
[39] Kedmi R, Ben-Arie N, Peer D. The systemic toxicity of positively charged lipid nanoparticles and the role of Toll-like receptor 4 in immune activation. Biomaterials 2010;31:6867–75.
[40] McAllister CS, Samuel CE. The RNA-activated protein kinase enhances the induction of interferon-beta and apoptosis mediated by cytoplasmic RNA sensors. J Biol Chem 2009;284:1644–51.
[41] Thimme R, Bukh J, Spangenberg HC, Wieland S, Pemberton J, Steiger C, et al. Viral and immunological determinants of hepatitis C virus clearance, persistence, and disease. Proc Natl Acad Sci USA 2002;99:15661–8.
[42] Bukh J. A critical role for the chimpanzee model in the study of hepatitis C. Hepatology 2004;39:1469–75.
[43] Zhu Q, Oei Y, Mendel DB, Garrett EN, Patawaran MB, Hollenbach PW, et al. Novel robust hepatitis C virus mouse efficacy model. Antimicrob Agents Chemother 2006;50:3260–8.